



Curtin University



DFN Team report

SpaceX debris Analysis from fall in NSW in July 2022

29 October 2023

Table of Contents

Table of Contents	2
Executive Summary	3
1. Introduction	4
1.1 Background.....	4
1.2 Overview	4
2. Accompanying Deliverables	4
3. Re-entry Review of Data	5
3.1 Known fragment locations.....	5
3.2 Atmospheric data	6
3.3 Weather radar data	6
4. Atmospheric Modelling	6
4.1 4D Data Product Description	7
4.2 Vertical Weather Profiles.....	7
5. Analysis and Strewn Field Predictions	8
5.1 Radar data.....	8
5.2 Provided Trajectory and Recovered Pieces.....	12
5.3 Alternative Sources of Data	13
5.4 Synthesis.....	14
6. Implications/recommendations	16
6.1 Spacecraft Behaviour	16
6.2 Ground fragments	16
6.3 Future events.....	17
Acknowledgments	17
References.....	17

Executive Summary

At around 7am on the 9th July 2022, a fireball and sonic boom from re-entering debris was reported by multiple witnesses in NSW. The Desert Fireball Network (DFN) team have 10+ years of expertise in observation and modelling of objects entering the Earth's atmosphere. Although it was not within the range of dedicated DFN cameras, the team were able to query all available datasets to estimate extent of the strewn field on the ground. The greatest hurdle was the lack of data on the fireball trajectory itself, altitude of re-entry, or break up history.

Signatures were however found in doppler weather radar data, usually used to monitor rain. Scans from radar are only every 5 minutes, and larger objects, such as the ones recovered so far and appearing in the media, would have escaped detection. Signatures were spotted for likely kg-sized objects and dust at 35-50 km altitude. This was the only dataset that 'observed' a part of this re-entry and fall.

A bespoke atmospheric wind model was calculated by the DFN team for the fall window (time and space). These winds are able to push the lightweight spacecraft materials significant distances. Heavy objects are less affected, and recovered pieces are close to the proposed ground track given by SpaceX. The nominal affected area by the radar-detected mm-sized dust particles covers nearly a 6000 km² area. Although there is no impact risk to humans, this area does reach Namadgi National park, and several lakes. The moderate kg-sized pieces detected in radar are also significantly affected by winds. Natural objects, with their high densities, usually land within 300 m of a fall line, these moderate pieces are detected by radar 10 km NE of the ground track fall line, and predicted to have landed up to 25 km off. This sideways scattering shows the significant effect of winds on light weight space debris for fall and risk analyses, and indicate there is likely to be many more pieces to recover to the NE.

The distribution of recovered pieces along the fall line is also significant. The 30 km separation between recovered fragments is inconsistent with a single breakup event. This indicates there was a likely a continuous shedding of material as the spacecraft re-entered. Re-entering debris is designed in this way, with the aim of vaporising the majority of the material, and any remaining pieces should be small. Without other sources of data, the altitude of breakup cannot be assessed, which would have given us a great deal of information on how and why such large pieces made it to the ground.

Due to the sensitivity to wind effects, and the likely cascading break-up, the potential strewn field is significantly larger than one expected for natural objects. This event is over a sparsely populated area, and could have been problematic over an urban area. If there was toxic or nuclear material involved, the affected area would have been significant.

As the problem of space debris becomes more prevalent, it will become increasingly important to monitor these re-entry events. The re-entry of a Soyuz capsule over VIC/TAS in August this year attests to that. The ideal method of monitoring space debris re-entry for the future is a dedicated network that can provide a trajectory solution, and assess the point at which the debris transitions from burn-up to free-fall. The height and speed of the debris at this point is critical to assessing the full impact. It would also have the capability to identify fragmentation points. Although Australia is large, the majority of its population is concentrated to the coastlines. Covering the Australian coast with a dedicated network is feasible, and a plausible trade off. However, one should also consider other criteria of significance, even in areas of low population density – such as indigenous or world heritage, and other protected areas.

Multiple actors beyond the DFN team operate in this field; the DFN team are working on integration of different sensors into their pipeline to facilitate analysis of such events, and to promote sensor fusion between actors, a common format for data input could be studied, proposed, and standardised. This would enhance collaboration and data fusion across the various priorities of civil/defence/research for these events.

1. Introduction

This report details an analysis and discussion of observations of the semi-uncontrolled re-entry of the SpaceX crew Dragon-1¹ trunk section over Australia/New South Wales in August 2022, by the Curtin University Desert Fireball Network team.

1.1 Background

Curtin University's Desert Fireball Network (DFN) team have 10+ years of expertise in observation and modelling of objects entering the Earth's atmosphere, predicting fall areas, and recovery of surviving objects. For the DFN project, specialist camera systems and purpose-built high-precision wind modelling software are used within trajectory models to predict constrained fall areas. For landed object recovery (with a scientific focus on meteorites), surveying using drones and apply machine learning techniques can automatically detect anomalies in images.

Although the DFN did not directly observe the SpaceX re-entry, this case is similar to natural events the team has analysed in the past, and the team have lent their expertise to reviewing and collecting data from various sources. They have used a suite of purpose-built tools to analyse the fall and provide the best view of SpaceX entry available to them.

1.2 Overview

The available data and the re-entry sequence is reviewed, followed by details of methodologies for atmospheric and dark flight modelling. The final section provides discussion and conclusion from the analyses, and discusses implications and recommendations for future re-entry events.

2. Accompanying Deliverables

- Weather model simulation product
 - a. 4 dimensional model (space + time) of atmospheric conditions, up to 30 km altitude (temperature, pressure, density, relative humidity, wind strength, wind direction) at the time of SpaceX debris re-entry.
File format: WRFOUT NetCDF. 4 files, 37 GB total
 - b. Vertical weather profiles at re-entry location and time
File format: csv, 50kb total
- Google Earth KMZ file that includes layers for radar returns, fall predictions of the larger material detected, and extent of affected areas that could be searched for potential debris.
File format: kmz. 1 File, 1MB total

¹ <https://www.nasa.gov/crew-1>

3. Re-entry Review of Data

At around 7am on the 09 July 2022 (21:00 08/07/22 UTC), a fireball and sonic boom from re-entering debris was reported by multiple witnesses in NSW. The fireball was travelling from North-West to South-East. This was later confirmed to be from the SpaceX mission Crew Dragon-1 (Figure 1), where the entering object was the 'trunk'. This disposable part of the Dragon capsule was separated from the crewed section prior to the controlled re-entry of the crewed portion of spacecraft (Seedhouse 2016).

The Desert Fireball Network team have custom built software to integrate and analyse the fall of meteoroids to the ground. For objects observed during bright flight, this gives a last known position, and with DFN systems, a known velocity (Howie 2017). However, in this case, there is no record of the bright flight trajectory or break up history, and alternative data sources must be investigated, coupled with the locations of known fragments.

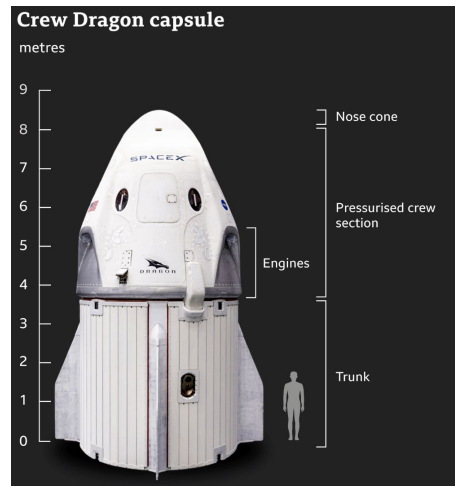


Figure 1 - Dragon capsule diagram, showing trunk and crewed capsule (Source: SpaceX)

3.1 Known fragment locations

The red line in Figure 2 is the ground projection of the SpaceX provided orbital trajectory. We would expect to see larger objects falling close to the line downrange (South-East), while smaller objects would be blown off the line and further up-range (North-West) if it is representative of the fall. Soon after the fireball event, debris was found and reported by various media sources. To date, three major pieces have been located (Figure 2), and matched to various dragon trunk components, as described in ASA (2023). It is likely that other pieces have been found and not reported, and that other pieces remain undiscovered.

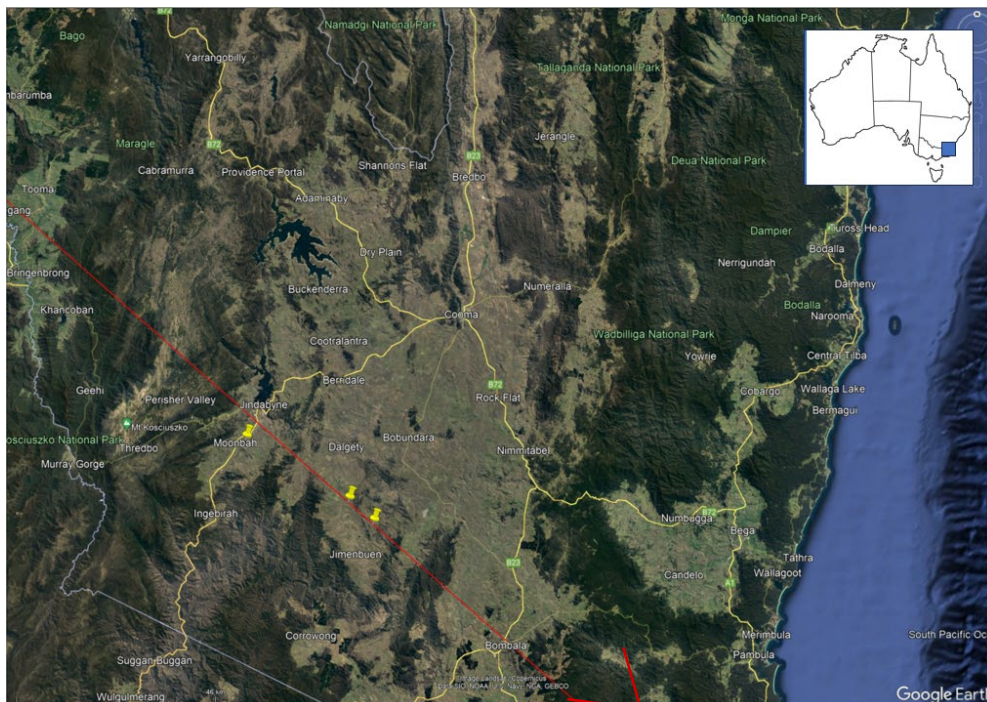


Figure 2 - shows the predicted orbital path of re-entry of the spacecraft (red line) entering from North-West toward South-East, and the three recovered major fragments (yellow markers).

3.2 Atmospheric data

After sufficient deceleration, re-entering objects lose enough energy that the fireball phenomena ceases. During the following 'dark-flight' descent through the stratosphere and troposphere, the atmosphere is highly variable. Upper atmosphere winds and density variations can significantly affect the fall of surviving space debris to the ground; impact positions can be shifted by several kilometres. In particular, upper atmosphere phenomena such as jet streams are the major drivers of how the fall line is shifted relative to an analysis without considering winds.

Modelling the fall of space debris through the dark-flight, or non-luminous phase requires high precision wind modelling. The DFN team uses a custom version of the NCAR atmospheric modelling system Weather Research and Forecasting software (WRF), incorporating real-world data (such as balloon flights), to model atmosphere dynamics. It extracts data relevant for the dark-flight scenario, producing a 3D data matrix for the suite of fall times.

3.3 Weather radar data

Weather radars operated by the Bureau of Meteorology (C or S-band) are designed to reflect off precipitation but can also ping off falling material such as meteorites and space debris. This capability has led to the successful recovery of meteorites in the past, and most recently by the DFN team in 2022 (Devillepoix et al., 2022, Anderson et al., 2023). The SpaceX event produced distinctive signatures in doppler weather radar data from the Captains Flat radar station south of Canberra (Fig. 5), at multiple altitudes and during several revisits. At high altitudes (>20 km), these signatures were isolated from other typical sources of radar reflections (precipitation, planes etc.), and consistent with an extended field of debris pushed by the wind. However, without a terminal bright flight point from which to model, estimating the size and shape of the objects detected is non-trivial. Here we use a Monte Carlo approach to trial different size, shapes and densities, and model their fall to the ground, incorporating the custom atmospheric model. The resulting product of dark flight traditionally aims to predict a likely search area for a meteorite. The most basic result is a fall line— a ground plot showing a line giving fall positions for a given range of proposed masses. For searching, of greater use is an impact probability scatter plot or heat map, where multiple scenarios are calculated for ranges in shapes/densities/winds.

4. Atmospheric Modelling

To predict the atmospheric properties, the DFN uses the NCAR atmospheric modelling system WRF version 4, with ARW dynamic core (Skamarock et al. 2019; <https://doi.org/10.5065/D68S4MVH>), initiated with NCEP FNL (Final) Global Tropospheric Analysis dataset (<https://rda.ucar.edu/datasets/ds083.2/>). The WRF is a forecast model that incorporates real-world data to model atmosphere dynamics, capable of being initialised from a global data set to generate mesoscale results at high spatial resolutions suitable for inputs into a dark-flight calculation. The WRF software generates a weather simulation product as a three-dimensional data matrix in a latitude/ longitude/height cuboid around the bright-flight endpoint. From the model, grid values are extracted for the atmospheric properties of relevance to trajectory modelling. This includes the pressure, density, temperature, relative humidity, and horizontal wind speeds as a function of height, latitude, and longitude (in u, v coordinates)

The WRF data cuboid is not necessarily north–south oriented and wind values must be extracted. Local verticals may also need to be corrected. For darkflight modelling of trajectories, this is incorporated into the calculation.

For convention in our analyses, we define wind directions in degrees, with north = 0, east positive, with a positive wind magnitude in the direction of wind travel, not the wind's origin.

As we are interpolating the past state of weather rather than forecasting, we can extract a physical model of the atmosphere based on observations both before and after the event, using

the archived data from the NCEP FNL Operational Model Global Tropospheric Analysis online data sets. These contain snapshots of global weather conditions every 6 hours.

The modelling case uses 4 nested domains, from level 1 (4860x4860 km, 180x180 cells with 27km resolution) down to level 4 nested domain with resolution 1km of size 337 x 337 cells. Due to the stochastic nature of the WRF numerical modelling software, slightly different results are produced each time it is run, even with the same input data, but the model outputs do not provide any error analysis. To resolve this lack of defined error bars, we initiated several models using different archived global snapshots up to 24 hours before the time of the re-entry (8 July 2022, 21:00 UTC; Table 1).

Four runs covering the were performed, starting the weather simulation at different times before the incident. Each run is stored in a single file, please refer to Table 1. We run four models and compare the results in order to find out the stability of the weather situation (Towner et al. (2022)).

4.1 4D Data Product Description

The provided 4D data is level 4 with resolution 1km for area 337x337 kilometres around the central point of coordinates: LAT = -36.30938, LON = 148.1371.

The weather model product includes a number of parameters, of which wind speed components, pressure, temperature, and relative humidity at heights ranging up to 30 km are applicable for the re-entry trajectory modelling.

The WRF model output files are in NetCDF format V4 and contain 4D matrix of weather data for the duration of the simulation (weather parameters at latitude, longitude, height and time). More details on the NetCDF format can be find in the user guide (<https://docs.unidata.ucar.edu/nug/current/>)

Table 1: WRF model product files

File	Modelling start time UTC	Modelling end time UTC
wrfout_d04_2022-07-08_00:00:00	8 July 2022, 0:00:00	8 July 2022, 21:30:00
wrfout_d04_2022-07-08_06:00:00	8 July 2022, 6:00:00	8 July 2022, 21:30:00
wrfout_d04_2022-07-08_12:00:00	8 July 2022, 12:00:00	8 July 2022, 21:30:00
wrfout_d04_2022-07-08_18:00:00	8 July 2022, 18:00:00	8 July 2022, 21:30:00

4.2 Vertical Weather Profiles

Four vertical profiles were extracted from the 4D data matrix. These are provided in a widely used and simple csv format and include primary and derived parameters, ready for use for simulation of dark phase of the re-entering fragments trajectory. The profiles were extracted at coordinates LAT = -36.30938, LON = 148.1371 and time 2022-07-08, 21:30:00 UTC.

Table 2 describes the meaning of the parameters essential for dark flight ballistic modelling. These are shown in Figure 3, and as wind profiles overlap, indicates fairly stable weather and reliability of the model. This will likely reflect in a low variation in the predicted fall area from the Monte Carlo statistical analysis due to the winds, as discussed in the following section.

Table 2: Parameters used for dark flight simulation		
Parameter	Meaning	Units
height	Height (for pressure level used in the model internally)	[m]
temperature	Air temperature at height	[K]
pressure	Air pressure at height	[Pa]
relative_humidity	Relative humidity at height	[%]
wind_horizontal	Wind speed (scalar horizontal component of the wind) at height	[m/s]
wind_direction	Wind direction at height (easterly = 90° = blowing from East)	[deg]
wind_east	East-West component of the wind at height	[m/s]
wind_north	North-South component of the wind at height	[m/s]
wind_up	Vertical component of the wind at height	[m/s]
density	Atmospheric air density at height (calculated from pressure, temperature and relative humidity)	[kg/m ³]

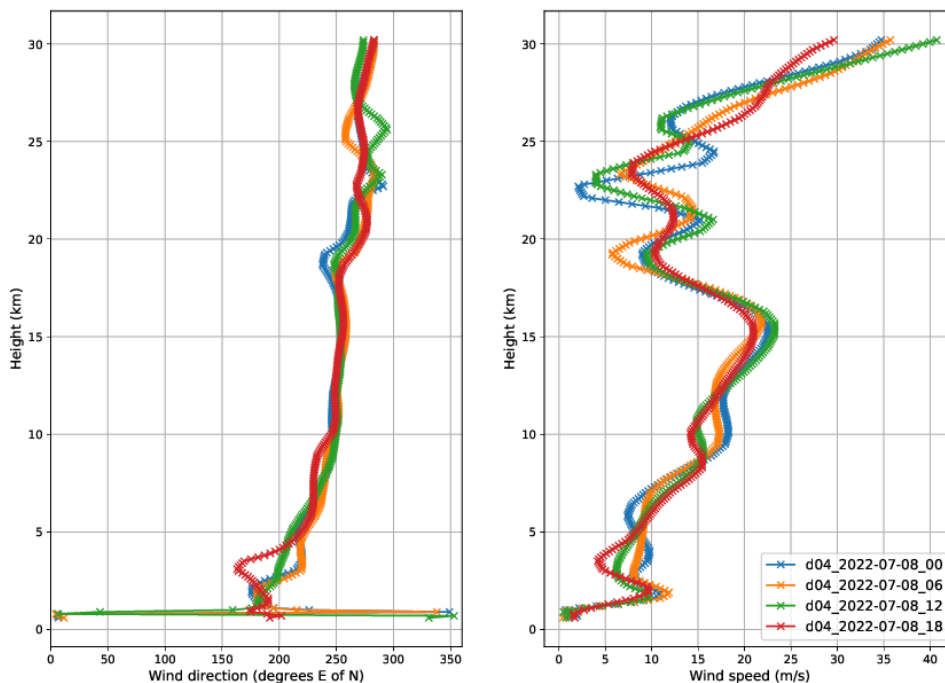


Figure 3 - Comparative plot of wind profiles, showing direction and speed as a function of height.

5. Analysis and Strewn Field Predictions

5.1 Radar data

Radar data is available from the doppler radar station at Canberra (Captains Flat) in S-band and Wagga Wagga in C-band, taken at 5 min interval scans. The large recovered objects are likely to have fallen very quickly to the ground (for example, 100 kg piece would have fallen in around 1.5 minutes). This makes it not impossible, but unlikely that these would be captured in the weather radar data. However, there is a good chance that moderate sizes were captured, and small particles may have been captured across multiple scans. For each scan, there are multiple 'sweeps' available, each corresponding to different elevation angles from the radar station. Depending on the distance from the station, radar returns will correspond to objects at different altitudes. For example the Captains Flat radar, there are 12 sweeps available for each time, with Sweep_00 observing the highest at 32 degrees above the horizon. This would correspond to

reflections near our fall zone at around 70 km altitude. Sweep_12 observes only 0.5 degrees above the horizon, and suffers from noise and interference from topography.

No visible returns were seen in any scan or sweep from the Wagga Wagga doppler radar station up range. For Captains Flat, scans at 2100-2110 UTC show little, apart from normal cloud responses and background noise that is typical of radar data.

The scan at 2115 UTC shows a prominent streak in sweeps 1 and 2 (Figure 4), and we are able to see distinct debris signatures down to sweep 7 (4.7 deg; material at ~10 km altitude).

The 2120 UTC scan also shows a streak, at lower altitude and shifted eastwards, with similar structure to the 2115 UTC high altitude streak. This potentially could correspond to the downward shift of falling small objects between scans, with a sideways shift that matches the direction of the prevailing westerly winds. A few returns are still captured at 2125UTC, though later scans from show no obvious features beyond the typical background noise. Note: see attached KMZ file for radar returns from Captains Flat.

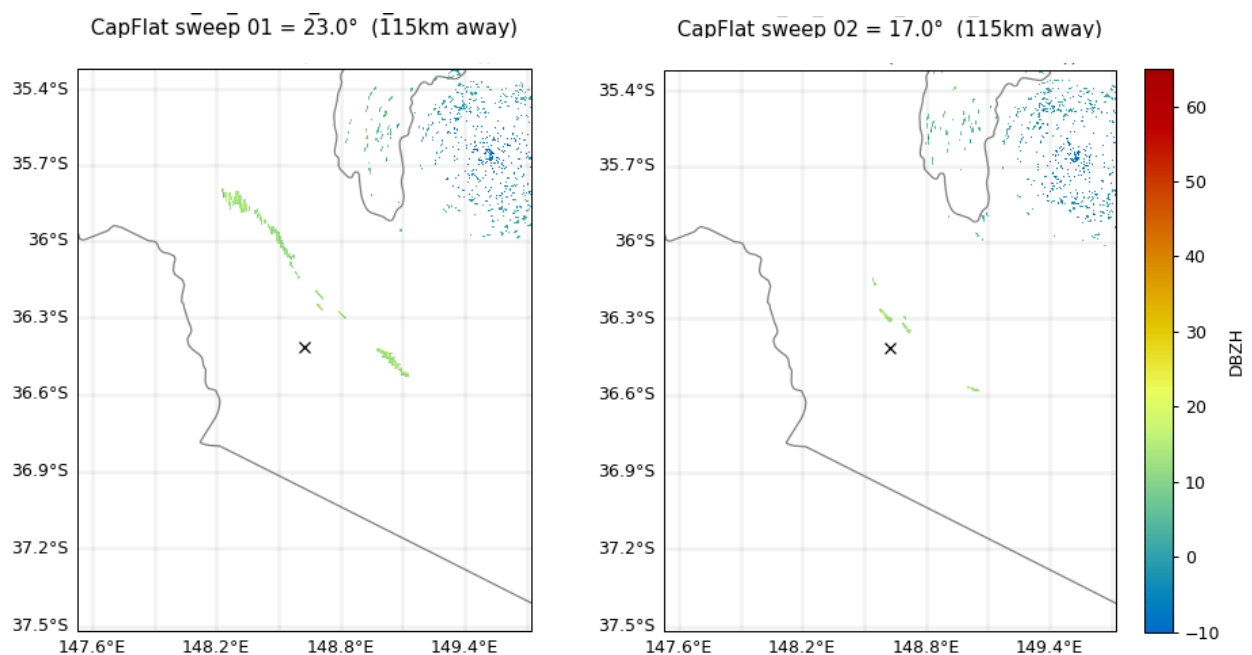


Figure 4 – Doppler weather radar reflectivity from Captains Flat at 21:15 UTC on 8th July 2022. Left shows Sweep 1 (23 degrees above the horizon from radar station), while right shows Sweep 2 (17 degrees above horizon). "X" is placed at the town of Jindabyne, roughly on the predicted re-entry line. Also note there are some small returns near the radar station itself in the North East. These are common to all scans and sweeps and are most likely genuine meteorological phenomena, such as cloud.

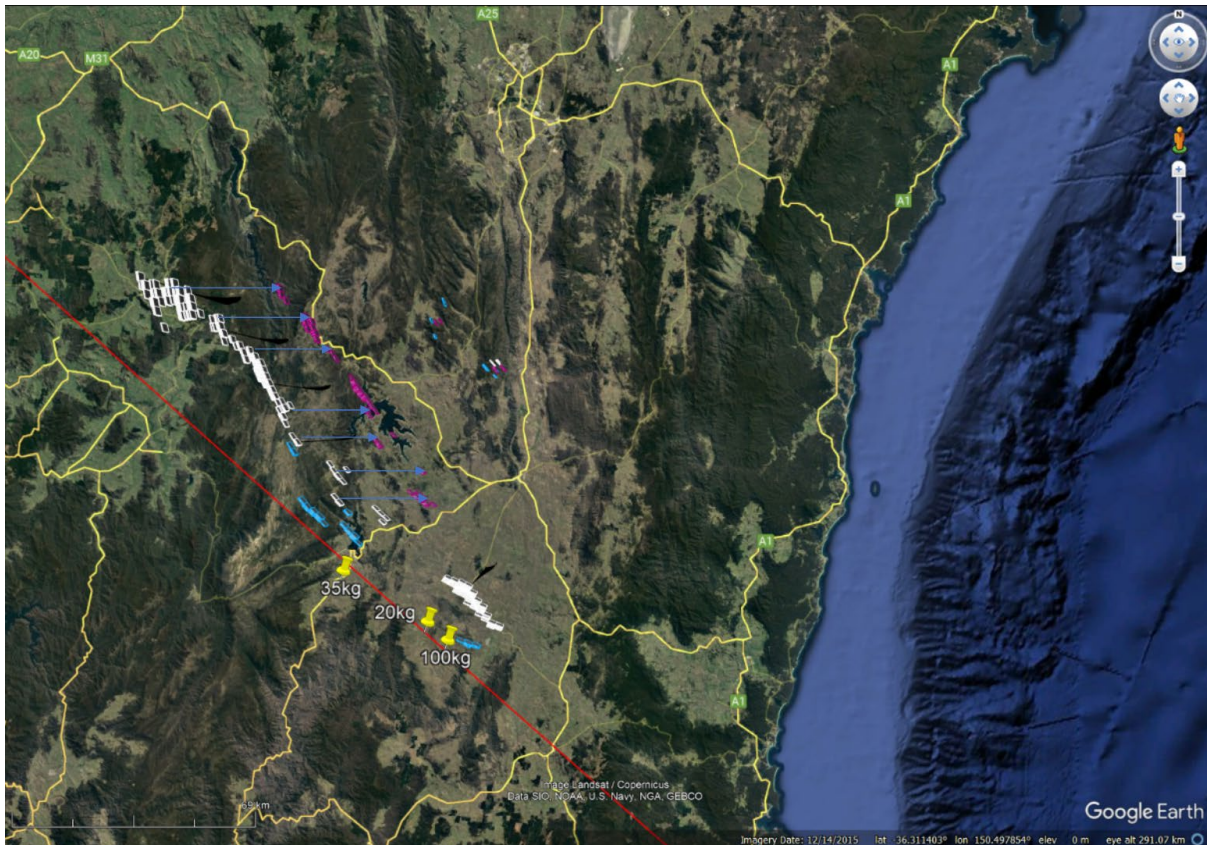


Figure 5 – Details of doppler radar returns; see text for detailed description

We have converted radar returns from Captains Flat scans/sweeps to blocks on a KMZ. These are shown in Figure 5. Here we have also plotted recovered pieces in yellow. The red line is the ground projection of the SpaceX provided orbital trajectory. We have coloured the radar return signatures by scan and sweep. Returns from the 2115 UTC scan, are white from high altitude returns of sweep 1, and light blue from the lower scan of sweep 2. The 2120 UTC scan, 5 minutes later, are coloured purple for sweep 1. Blue arrows show the potential drift eastward and down of particles from 2115 to 2120, although it is very difficult to say for certain if these are the same objects. If these are not, the cloud of fragments being detected by the radar indicates a very large quantity of debris.

If these were to represent the same objects across sweeps, from the movement of the streak spacing and timing, we can use this to roughly approximate the size and cross-sectional area of the object seen by radar, by correlating 'clumps', and structure within the streaks. This gives a basic estimation of some of the size ranges seen by weather radar, which has been a longstanding unknown, and is useful for future falls.

The governing equations for this estimate are:

1) assuming a spherical object

$$m = \rho \frac{4}{3} \pi r^3 \quad \text{Equation 1}$$

Where m is mass, ρ is the density of object (assumed as 1000 kg/m³ as typical for spacecraft average structure), and r is sphere diameter.

2) terminal velocity of falling:²

$$V = \sqrt{\frac{2mg}{\rho_a A C_d}}$$

Equation 2

Where V is the velocity, g is the Earth's gravity (9.81 m/s²), ρ_a is the atmospheric density (about 0.002 km/m³ at these altitudes), A is the cross-sectional area (πr² for a sphere), and C_d is the drag coefficient (0.51 for a sphere under these conditions).

Combining and rearranging these equations to extract mass, and hence diameter, the values in Table 3 are generated using the estimates derived from Figure 1.

Table 3 : First two columns show the derived altitude for each radar return for two different scan times (both Sweep_1). Following columns are derived values from the fall and sideways drift of particles between these two scans, assuming they are representing the same objects.

2115 UTC altitude (km) (Figure 5 – white)	2120 UTC altitude (km) (Figure 5 – purple)	Derived horizontal speed (m/s)	Derived vertical speed (m/s)	Derived particle diameter (mm)
49237	39701	98.16	31.79	0.73
46219	38400	83.61	26.06	0.49
43910	37300	73.66	22.03	0.35
43308	36601	81.84	22.36	0.36
43809	37601	77.62	20.69	0.31
42606	36401	80.28	20.68	0.31
44110	38400	76.70	19.03	0.26

From the sideways drift, and time taken to fall the distance shown, it is clear that the white→purple radar returns are from very small, fine objects, with the calculated diameters shown in Table 3, of sub-mm. Composition is unknown, but most likely metallic/glass/carbon fragments corresponding to the components within the Dragon trunk (Seedhouse 2016). These particles would drift and disperse as they fell lower (the lowest observed elevation is still ~ 36 km), and may travel significant distances. The horizontal speeds are surprisingly large, but winds above 30 km are not modelled by the WRF. If the fireball trajectory were known, we could model the upper atmosphere winds using NRLMSISE-00, and get a better understanding of the influence. This is an empirical, global reference atmospheric model of the Earth from into space. Without knowing the breakup, these small fragments that are still suspended in the atmosphere 30 minutes later, are already widely dispersed. Their presence to the North could also indicate that there was major fragmentation earlier in the trajectory, and pieces may be recoverable up-range. Such particles will eventually fall to the ground, and enter the ecosystem, but will pose no impact hazard.

Separate to these small objects, in the 2115 UTC radar scan, the lower altitude returns are more likely to correspond to larger fragments (Figure 5 –blue symbols), as these objects have fallen further compared to the upper streak in the same amount of time. Consistent with this is the fact they are further down the track (toward the SE), as is expected for larger objects. It is unlikely that the blue returns correspond to recovered objects, as their altitude at 2115UTC is still too high (and therefore travel speed to the ground from the likely breakup too slow to correspond to such large objects). These are more likely to be from 10s of grams or smaller objects based on the timing.

² https://en.wikipedia.org/wiki/Terminal_velocity

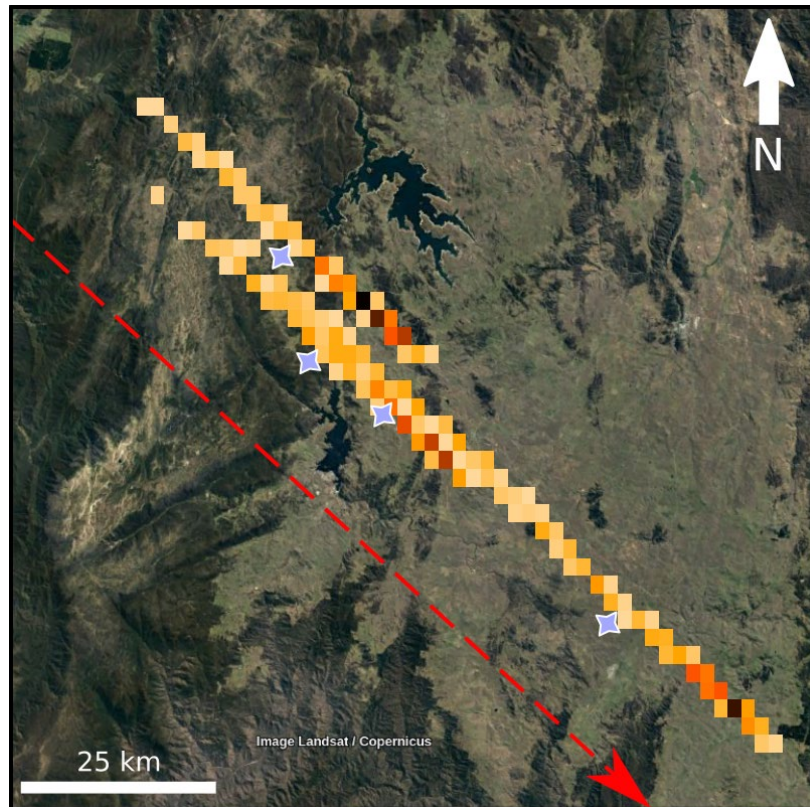


Figure 6 - heatmaps for predicted possible fall areas of four larger radar returns objects in 2115 UTC Sweep 2 (blue stars)

In Figure 6 we show the predicted fall positions derived for the larger radar returns only. This is using DFN software to carry out dark flight predictions, calculating the fall trajectory of hypothetical objects given a starting condition and atmospheric model. See Towner et al. (2022) for full details, and links to the available code. This figure represents a Monte Carlo analysis, of 500 scenarios for each object, allowing the winds to vary by $\pm 5\text{m/s}$ in each layer, variation in shape from 'sphere' to 'brick', variation in mass from 0.5 to 2 kg, variation in initial position and velocity of 200 m, 100 m/s respectively. These are relatively generous values compared to typical fireball operations, as the radar data provides limited insight on the nature of the objects. Fall lines are well constrained close to parallel to the orbital track, showing that winds are not a major factor, and the uncertainty is driven by the choice of projectile properties. Ground dispersion is typically 5-800 m across track, and 20-30 km long, so a relatively large area.

5.2 Provided Trajectory and Recovered Pieces

The launch capsule manufacturer has provided a re-entry trajectory. No atmosphere drag is included in this trajectory, so as a theoretical construct it passes over the fall area at heights of about 200 km. The ground projection of this trajectory passes almost exactly over the recovered larger pieces (200 - 300m off track), which is surprisingly close to the actual recovered fall positions. This is consistent with these larger objects separating from the main body at relatively late within the breakup; if they had separated earlier, they would be more off track, and further NW.

Three large known pieces have been reported to date, at locations shown in Figure 2. All pieces are large, but of significantly different shapes (which would alter their aerodynamic properties and hence atmospheric trajectory). All are close to the predicted incoming trajectory, although it is not clear how much active ground searching has been carried out away from the prediction. Other pieces may have been recovered, but not yet documented.

Using the known locations of the larger recovered objects, it is theoretically possible to back calculate the entry trajectory, but this is non-deterministic as the switch in influence from a free-fall object to a ballistic orbital path is still unknown.

However, the separation of these large pieces is unusual, and inconsistent with a common breakup point. Typically, larger objects that originate from the same breakup event may have separation of a few kilometres due to winds. This could be accentuated by the significantly different aerodynamical shapes, but the ~35km difference along track between the 35 – 100 kg recovered objects implies individual break off events, rather than one breakup/failure. As such, other unrecorded events may have occurred along the orbital path.

Of note is the northern most piece which is nearly 5 km west of the orbit line. This western off-track distance cannot just be a result of the winds, as the prevailing winds will act to push objects to the east, so the object must have received an initial 'kick' to the west from its breakup event.

5.3 Alternative Sources of Data

Data sources capable of feeding into re-entry observation, triangulation and strewn field predictions that have previously been fruitful for meteorite recoveries:

Observation method	Comment and limitations
Optical	<p>Optical sensors have a wide range of capabilities depending on the sensor, time resolution and access to calibration data. They are limited to bright flight trajectory (fireball) and by weather.</p> <p>Different levels of optical systems include:</p> <p>Dedicated camera network such as the Desert Fireball Network can provide high precision position and timing, all sky so can cover large areas, currently limited to night-time.</p> <p>Fixed casual video/images such as a from a security camera is lower resolution and usually struggles with precision timing of frame capture. Calibration can be difficult if resolution limits ability to see stars at night.</p> <p>Non-fixed casual video/images such as dashcam or smartphones are very imprecise as calibration cannot easily be done. They are serendipitous recordings, usually as a response to an event and so rarely detect the beginning of an event.</p>
Doppler weather radar	<p>Can see small things falling, but is too infrequent to guarantee capture of larger objects. 24 hr coverage, but over a very limited area (up to 150 km from a station). Limited number of sites over Australia that are mostly over population centres. Poor weather introduces noise.</p>
Other radar (military)	<p>Issues with access to data</p>
Seismic/ Infrasond	<p>Are able to capture the sonic boom from the trajectory shock wave. It has 24 hour coverage, and can detect events within ~250 km (potentially further for infrasond, but no test cases to check). Very limited spatial resolution and at most can confirm an event occurred (and order of magnitude distance). Generally hard to detect events in the large noisy datasets in real time, but they can be found in the data afterwards.</p>

Earth observation satellites	Can have multispectral sensors, potentially identifying material properties of debris. For example, JAXA's Himawari. They are low spatial resolution, and mostly limited by infrequent observations.
AMOS	Dedicated scientific instrumentation to observe the spectra of a fireball. It provides details of the observed chemistry involved in an event, but only a few observatories exist.
CNEOS ³	Detections posted from the US DoD ballistic warning system. Limited to events greater than 0.7kT TNT equivalent energy (insensitive to low velocity/energy events). High time sensitivity, but low spatial sensitivity.
Drone surveying	Detailed surveying and searching of a strewn field after landing/impact

The DFN investigated the following alternative data sources that may have captured data from this event.

The **Himari weather satellite** captures visual/near infrared global observations of the Earth over Australia/Japan every 10 min. In the past, it has observed transient dust clouds from very large meteor entries. Data taken around this event show no features of interest. This is disappointing, but not unexpected, as the global images is relatively low resolution, and only captured every 10 minutes.

The **CNEOS database**³ displays US NASA/DoD observations of atmospheric fireballs/explosions. The system is designed primarily to detect missile launches and nuclear explosions greater than 0.07kT of TNT equivalent, and only detects the largest atmospheric impact events. It is therefore relatively insensitive to re-entries (in particular, ones that do not end in a single catastrophic airburst), and unfortunately nothing is reported that correlates with this re-entry.

As there were witness reports of a sonic boom, **seismic sensors** from the Australian National Seismograph Network were checked for signals. An extended signal was detected in the expected window from Young, NSW, indicating a ballistic trajectory source rather than airburst or fragmentation events. The signal was identified at 2022-07-08T21:07:30 which corresponds to a source distance of ~145 km. This is consistent with the proposed re-entry track 150 km away from Young.

Other military monitoring systems may have observed the entry and may be of interest to defence.

5.4 Synthesis

Without information such as the re-entry trajectory, entry speed, or final ablation point, it is very difficult to represent the full extent of the strewn field on the ground. Based on interpretation of radar data for fine to moderate sized objects, and the known recovered large pieces, we can build a picture of the likely strewn field area for the 'final' fragmentation event. Any cascading fragmentation earlier would likely have resulted in other objects falling up-range (toward the NW).

By carrying out darkflight calculations from the largest radar observed objects (Figure 5 –blue events), this indicates the likely (probably quite sparse) strewn field from the trajectory of smaller (kg and less objects). We don't expect larger objects to extend further NE as they will not be

³ <https://cneos.jpl.nasa.gov/fireballs/>

greatly influenced by the winds. The very fine particles seen in radar give the maximum North-Eastern extent of possible fall zone but such fine material would be unobservable on the ground, except by analytical methods such as soil studies. Larger fragments than the fine dust undoubtedly exist, but may not have been observed by radar due to the 5 minute radar sweep interval. As they would have been shed by the spacecraft during entry, these would be further up track to the NW.

No returns are seen in the radar to the South-West of the lower 'blue' returns, indicating that this is probably the western extent of significant falls. In previous work, (Devillepoix et al, 2022; Anderson et al 2023) ground radar has seen individual objects down to 300 g in one case, but below that single objects are too small for a detectable radar return.

The large, recovered pieces give the general maximum western extent, with the 35 kg item west of the orbit line implying that it is possible for items to fall slightly to the west. In previous meteorite recoveries, the maximum observed cross track distance is 4-500m, so it will be unlikely to be major falls to be further South-West than that.

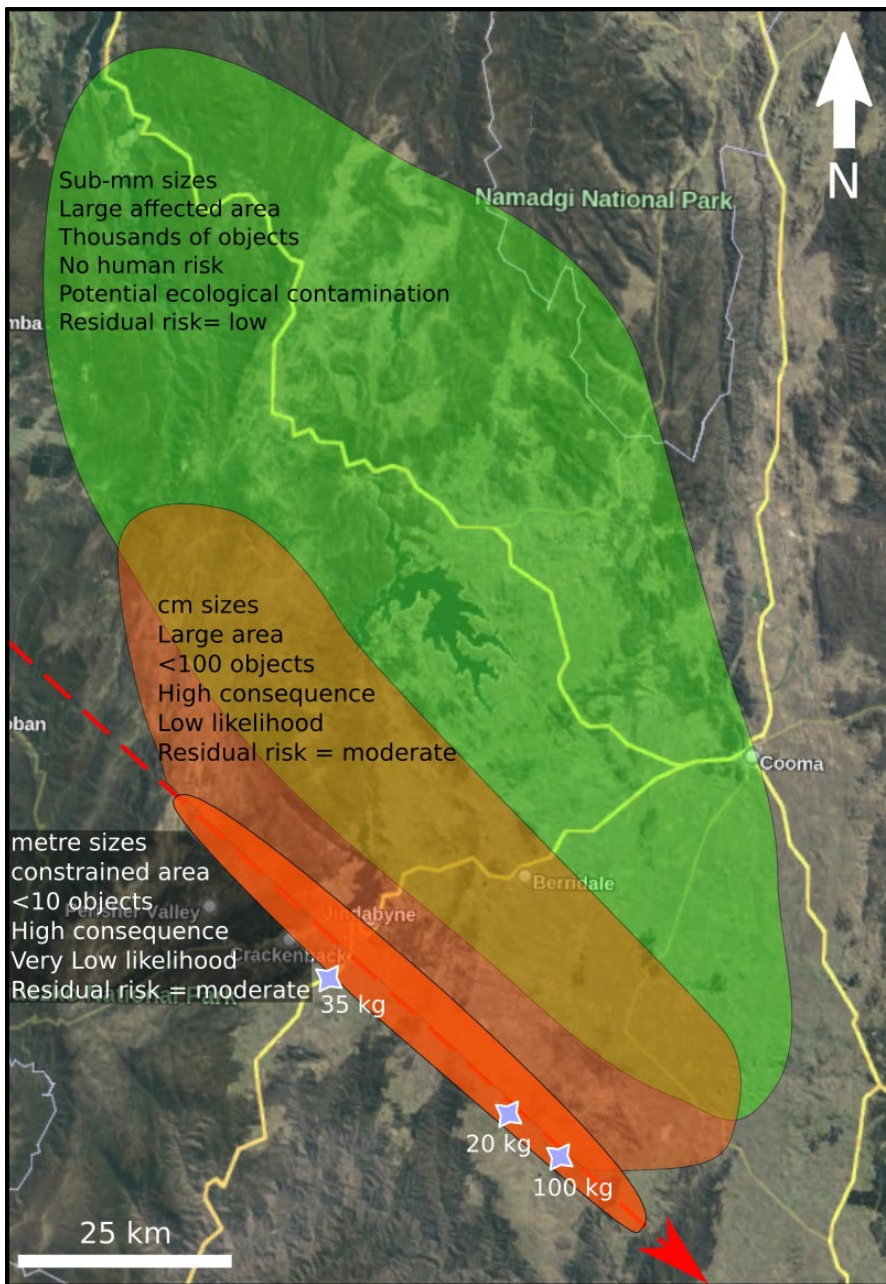


Figure 7 Shows areas affected by potential size classes of debris. The dark orange zone, very close to the orbital path, is for larger multi-kg objects. Orange represents the medium objects, corresponding to radar returns and possible larger fragments that may have fallen too quickly for radar detection. This area potentially extends to the NW (up-range) to coincide with the extend of the green area seen by radar. Green indicates the potential fine/small area, for sub-gram sized particles, although the number of particles per area is likely to be small, and patchy, depending on fine detail of local winds, topography etc. Blue stars represent recovered debris pieces.

6. Implications/recommendations

6.1 Spacecraft Behaviour

There is evidence for gradual breakup as designed, but clearly pieces made it to ground. NASA has a mandatory standard covering requirements for re-entry (NASA-STD-8719.14, sec 4.7)⁴, and it is not clear that this event satisfies those criteria. Without other sources of data, the altitude of breakup cannot be assessed, which would have given us a great deal of information on how and why such large pieces made it to the ground. Due to the sensitivity to wind effects, and the likely cascading break-up, the potential strewn field is significantly larger than those from natural objects.

6.2 Ground fragments

The lack of many multiple radar returns beyond what is seen in the East implies not too many extra major fragments. This is not unreasonable, as consideration of safe breakup criteria is a regulatory requirement for space capsule design and certification.

Searching for very small fragments would be unfeasible, given the large area and size range, and probably low number density. It would be interesting to see if very fine dust is detectable in soil/lake, would need a specialist environmental monitoring approach, starting with discussion with appropriate expertise about sampling strategy.

If not already searched, the areas along the orbit line, in particular to northwest would be the highest priority, and the best location for larger fragments. Based on the pieces found, and previous falls, surveying ± 500 m from line would be sufficient, and these should be easily detectable, as they would be up to 10's kg. It is unlikely there are any increasingly larger fragments to SE, as they would have been found already. Searching of fall line area would confirm the validity of the provided orbital trajectory, and ensure that any other large objects were recovered. Searching of the areas NE of the orbital track may recover smaller pieces, and this would provide more information concerning the break up and validity of the wind model, but such objects are not a major hazard if undiscovered.

One of the most cost-effective ways to carry out ground searching is by using UAVs (airborne drones). In the case of open ground and looking for multi kg fragments, quadbike is also effective as large areas can be covered quickly. For aerial drone searching, the DFN team has been developing next generation image recognition technology to locate meteorites fallen on the ground in drone survey imagery. The world-first proof of concept was successfully demonstrated in Dec 2021 (Anderson 2022). Although the artificial intelligence (AI) was trained to specifically find meteorite-looking rocks, it is able to highlight all anomalous objects in the images. The machine learning used is based around a Convolutional Neural Network algorithm, trained generally on a background dataset, and then enhanced by onsite training in the specific location, so such searching requires time on site initially to train the software on the background vegetation. The area coverage rate depends on size of objects of interest. When searching for something the size of a golf ball, such as the 2021 search, the drone is able to cover 5 km² at 1.8 mm/pixel in 2.5 days. On-site data processing can raise objects of interest. Considerations would need to be made for such things as terrain variations (farmland vs bushland), tree canopy coverage, and landowner permissions.

Drone coverage is typically 1 km²/day (dependent on likely mass range of interest, which determines ground resolution needed which sets ideal drone altitude), which for full high priority fall line would be approximately 2 weeks of field searching

⁴ <https://standards.nasa.gov/standard/nasa/nasa-std-871914>

For larger objects, aerial searching may be more cost effective, although with the current technologies, drones are generally cheaper – one just flies the drone higher, and cover more ground per day at lower resolution (subject to regulatory constraints such as airspace controls).

6.3 Future events

Australia is a large place, and in this case the fall was in a sparsely inhabited area. There is the small chance of a future re-entry over a populated area, but this is beginning to increase as space debris becomes more prevalent. Australia also possesses valuable and protected natural environments, as well as cultural heritage areas and areas of indigenous significance. Due to its size, objects re-entering over sparsely populated remote regions go relatively undetected, with the possibility of ground contamination (as famously occurred with the uncontrolled re-entry of Skylab over WA in 1979).

To monitor these issues with confidence, observing capability is needed, be it with optical sensors or other sources such as in section 5.3. The ideal method of monitoring space debris re-entry for the future is a dedicated network that can provide a trajectory solution, and assess the point at which the debris transitions from burn-up to free-fall. The height and speed of the debris at this point is critical to assessing the full impact. It would also have the capability to identify fragmentation points. A Desert Fireball Network solution covering the Australian coast is highly feasible. Another option would be to deploy temporary stations along the ground track of a planned re-entry event in order to better understand the nature of breakup and quantify the risks.

There is value in collaborating with Defence in this area, particularly where they have existing radar and existing sensors, or looking to develop them. Data fusion across sensors, and developing a common data format for sharing of data could be considered.

Acknowledgments

We acknowledge the support of ASA in providing their initial observations and facilitating analysis.

References

- Anderson, S. L. et al (2022). Successful Recovery of an Observed Meteorite Fall Using Drones and Machine Learning. *The Astrophysical Journal Letters*, 930(2), L25.
<https://doi.org/10.3847/2041-8213/ac66d4>
- Anderson, S. L. et al (2023), Meteor(ology/itics) Unite!: Multi-Instrument-Enabled Discovery of a New Orbitally-Constrained Meteorite Strewn Field,
<https://ui.adsabs.harvard.edu/abs/2023LPICo2806.1884A>
- ASA (2023), PowerPoint analysis of major recovered items.
- Devillepoix H. A. R. et al (2022), Detecting Falling Meteorites with Weather Radars in Australia,
<https://ui.adsabs.harvard.edu/abs/2022LPICo2678.2888D>
- Howie, R. M. et al (2017). How to build a continental scale fireball camera network. *Experimental Astronomy*, 43(3), 237–266. <https://doi.org/10.1007/s10686-017-9532-7>
- Seedhose, E. (2016) SpaceX's Dragon: America's Next Generation Spacecraft, Springer Praxis Books, Switzerland, ISBN 978-3-319-21514-3
- Towner et al. (2022) Dark-flight Estimates of Meteorite Fall Positions: Issues and a Case Study Using the Murrili Meteorite Fall, <https://iopscience.iop.org/article/10.3847/PSJ/ac3df5>